Separation and Purification Technology 310 (2023) 123166

Contents lists available at ScienceDirect

Separation and Purification Technology

journal homepage: www.elsevier.com/locate/seppur

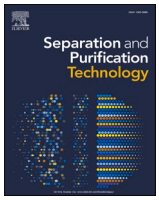

Analysis of hybrid separation schemes for levulinic acid separation by process intensification and assessment of thermophysical properties impact

Stefania Tronci [a], Debora Garau [a], Roumiana P. Stateva [b], Georgi Cholakov [c], William A. Wakeham [d], Massimiliano Errico [e,*]

[a] Università degli Studi di Cagliari, Dipartimento di Ingegneria Meccanica, Chimica e dei Materiali, Cagliari I-9123, Italy
[b] Institute of Chemical Engineering, Bulgarian Academy of Science, 1113 Sofia, Bulgaria
[c] University of Chemical Technology and Metallurgy, 1756 Sofia, Bulgaria
[d] Department of Chemical Engineering, Imperial College of Science, Technology and Medicine, London SW7 2BY, UK
[e] University of Southern Denmark, Faculty of Engineering, Department of Green Technology, 5230 Odense M, Denmark

ARTICLE INFO

Keywords:
Biorefining
Process modeling
Process intensification
Building block chemicals
Parameter estimation

ABSTRACT

From the time levulinic acid was listed as one of the top-12 building blocks for the sugars-high value compounds conversion, the interest in this compound increased. As part of its possible production route, the definition of viable separation schemes appears of paramount importance in the overall development of levulinic acid exploitation. Hybrid sequences where liquid-liquid extraction is followed by distillation were considered proving how the direct and direct -indirect separation schemes appeared to be the best alternatives in terms of total annual cost and environmental impact. These alternatives were further analyzed to improve their design by complementing the process simulator database with thermophysical experimental values. After obtaining a reliable design for the hybrid direct and direct-indirect configurations used as benchmarks, two intensified alternatives were generated. The first intensified configuration is classified as thermodynamically equivalent sequence, while the second one includes a divided wall column. For both, it was achieved a reduction of the total annual cost of 11% without any penalty for the environmental impact compared to the reference case.

1. Introduction

The chemical 4-oxo-pentanoic acid, commonly known as levulinic acid (LA), is a multifunctional compound including in its structure both a keto and a carboxylic acid group. In 2004 the U.S. Department of Energy published the report "Top Value Added Chemicals from Biomass" [1] and listed LA as one of the highest-valued bio-based chemicals and counted it among the top 12 building blocks obtainable from sugars and convertible into high-value chemicals. Subsequently, the interest in its synthesis and purification substantially increased. LA can be produced following a synthetic route from petrochemical-derived feedstocks, through the Pd-catalyzed carbonylation of ketones [2] or by conjugate addition of primary aliphatic nitro compounds to acrolein on an alumina surface and oxidation [3]. However, as anticipated by Reid in 1956 [4], "*although levulinic acid has been known since the 1870's, when many of its reactions were first established, it has never reached commercial use in any significant volume. Reason for its slow development probably are expensive raw material and low yield, excessive equipment cost for its production, and physical properties detrimental to easy recovery and handling*".

Regarding the cost of raw materials, considerable progress has been achieved since, starting from raw cellulosic feedstocks, LA can be obtained by sequential steps of acid hydrolysis. In particular, the reaction includes the dehydration of hexoses to 5-droxymethylfurfural (HMF) and its subsequent hydration to LA and formic acid [5–7]. The biomass selection will always be the first step, and of primary concern in any feasibility work on the recovery of the target component(s). For LA production, different feedstocks were reviewed by Morone et al. [8] and more recently by Di Menno Di Bucchianico et al. [9]. Together with the feedstock selection, the choice of the catalyst stands out as an important issue that affects the yield of LA. Moreover, whether a homogeneous or a heterogeneous catalyst or a combination of the two should be chosen, is a topic of great interest. Sulfuric, phosphoric, and hydrochloric acids are the most common liquid catalysts used. For instance, Fachri et al. [10] found an LA yield of 74 mol % using a 0.1 M solution of D-fructose treated with 1 M sulfuric acid at 140 °C. Regarding heterogeneous

* Corresponding author.
E-mail address: maer@igt.sdu.dk (M. Errico).

https://doi.org/10.1016/j.seppur.2023.123166
Received 31 October 2022; Received in revised form 9 January 2023; Accepted 9 January 2023
Available online 11 January 2023

catalysts, Woo Lee et al. [11] reported that the proton donor ability of the heterogeneous catalyst is less than that of the homogeneous catalyst, resulting in a lower yield of LA. This aspect leaves the immobilization of Brønsted acid sites on heterogeneous catalysts an open challenge for the research community. Alongside feedstock screening and the kinetic studies, the synthesis of efficient separation processes and their modeling represents a step of paramount importance in the overall process economy.

Taking as a reference well-established oil refineries, the separation and purification steps, usually performed by distillation, liquid–liquid extraction, crystallization, absorption, adsorption, and membranes, account for 40–50% of the total costs [12]. However, the case of bio-derived compounds is more complex. The target component is often dilute, and the occurrence of water and oxygenated compounds further complicates the phase behavior making it even more complex owing to the presence of azeotropes. Furthermore, thermal stability needs to be taken into consideration which limits the operating temperature. In the case of LA, and in particular, mixtures where the product dilution is lower than 20 wt%, the separation costs account for 60–80% of the total production cost [13]. The acid biomass hydrolysis typically produces a diluted stream containing 3–8 wt% LA, 1–5 wt% formic acid (FA), and 1–5 wt% furfural (F) [9]. Although LA itself does not form any azeotrope with the mixture components, the pair water-furfural forms a minimum-boiling, heterogeneous azeotrope at 97.8 °C and at a furfural content of 64.5 wt%, while the pair FA-water forms a maximum-boiling heterogeneous azeotrope at 106.8 °C [14]. Ordinary distillation is therefore not feasible for this mixture. However, liquid–liquid extraction has the potential to separate the water-rich phase from the solvent-rich phase containing LA, FA, and F. The latter can be further processed by distillation. For example, Seibert [15] proposed a separation process where F is used as the extracting solvent, then the extract is separated by a sequence of three distillation columns. LA is recovered as a bottom stream of the first column, the second column separates the F-water azeotrope as distillate that is recycled to the extractor feed, and a mixture of F-FA as residue. The two constituents of the latter are separated in the third column where FA is recovered as distillate and F as residue. These alternatives can be defined as hybrid schemes according to the definition provided by Babi et. al. [16] where a hybrid unit is considered an operation that enhances the function of one or more unit operations performing a task or a set of tasks through a new design of the unit operation or a combination of more than one unit operations.

Hybrid schemes where a liquid-liquid extraction is used to separate the aqueous phase were also applied in other bio-related separations, such as the acetone-butanol-ethanol (ABE) mixture [17–18], and bio-ethanol [19,20]. Details on the synthesis and intensification of those processes were reported by Errico [21].

Even though hybrid liquid-liquid-extraction assisted distillation appears as a viable alternative for the LA separation, challenges might still arise in the modeling. In particular, the necessity to supplement the separation models with experimental data appears particularly relevant for bioprocesses. The widespread use of process simulators has somehow underestimated this aspect since the user relies entirely on the in-built component databanks and/or estimation methods. The topic was discussed by Wakeham and Assael [22] reporting, among other examples, how the experimentally measured value of toluene's thermal conductivity changed over the years with a direct effect on the design equations of the unit operations where this value is used. Because toluene is a chemical used in several processes, its thermophysical properties both in the pure state and mixtures have been measured frequently and carefully and it is reasonable to rely on the data embedded in the process simulators for it. However, one cannot be so confident when new materials or hot topic components are constituents of a process system where their properties have either not been measured, or poorly measured. The substitute refrigerant R134a is an example of a pure material where this problem was initially acute [23] and the modern pursuit of the "hot topic of nanofluids" a more recent example [24].

With regard to LA, its physicochemical properties (density, dynamic viscosity, refractive index) at different temperatures and atmospheric pressure were reported by Ariba et al. [25]. Nikitin et al. [26] reported experimental data for LA including critical properties, heat capacities, thermal conductivity, and thermal diffusivities. The values were compared with those estimated by equations based on group contribution methods, and the results demonstrated that the critical pressure was underestimated by 23 to 24%. It is clear that good experimental data on the properties of LA and its mixtures with other compounds in the processes will not only enhance the databanks process simulators but will have the potential to improve considerably the process design of the unit operations used in the flowsheet synthesis.

In this study, the separation of LA produced through acid hydrolysis is considered using hybrid configurations where liquid-liquid extraction is combined with distillation. The results obtained with the default parameters of the process simulator Aspen Plus were compared with those achieved integrating into the component data banks, experimental data for the components LA, FA, F, and the design corrected accordingly. After the definition of a reliable design, different intensified alternatives including a divided wall column and a configuration with thermal coupling were considered to improve the process feasibility.

2. Review on hybrid separation schemes for LA separation

The configuration proposed by Seibert [15], reported in Fig. 1a, is often considered as a benchmark when alternative liquid-liquid extraction and distillation configurations are proposed. The possibility to recover LA from acid hydrolysate was also considered by other authors with the aim of comparing different solvents [27,28]. In this work, the analysis is limited to the case of F as extracting agent according to published studies on LA separation [14,29,30]. Nhien et al. [14], applying heuristic rules, proposed an alternative configuration shown in Fig. 1b. In particular, the separation order of the components was changed with the azeotrope water-F being separated in the first distillation column, the FA recovered as distillate in the second, and the LA as the residue of the third one. In this way, the authors reduced the reboiler duty associated with the high boiling point component and the corresponding total annual cost (TAC). The same authors [14] further improved the configuration of Fig. 1b in order to minimize the amount of F lost in the azeotrope. This was realized by introducing a decanter at the top of the first column to take advantage of the heteroazeotrope and recover an F-rich phase used as reflux and a water-rich phase as distillate. The recovery of F depends on the decanter cooling temperature and represents an optimization variable. The corresponding configuration is displayed in Fig. 2a.

This configuration was then used by the authors to generate an intensified top dividing wall column with a decanter configuration. Nevertheless, considering the synthesis procedure for intensified distillation columns, discussed by Errico and co-authors [31–35], there is a direct correspondence between the simple column sequences and the intensified alternatives. This connection highlights the importance of screening the subspace that includes all simple column alternatives. The conclusion appears even more relevant given the work of Alcocer-Garcia et al. [30], where multiple dividing wall configurations were proposed starting from the configuration reported in Fig. 2c. However, based on the number of components in the feed and following Thompson and King [36], there are five possible configurations as reported in Fig. 2, and they all should be designed and compared before proceeding with the generation of intensified structures. This task was achieved by Errico et al. [29] using a different set of purity requirements than those of Nhien et al. [14], and Alcocer-Garcia et al. [30]. These differences render a direct comparison of the results obtained impossible.

In this work, the set of configurations reported in Fig. 2 was designed with an emphasis on the setting of the decanter temperature and its performance depending on its position on the separation scheme. The design of the best configurations is repeated after integrating the process

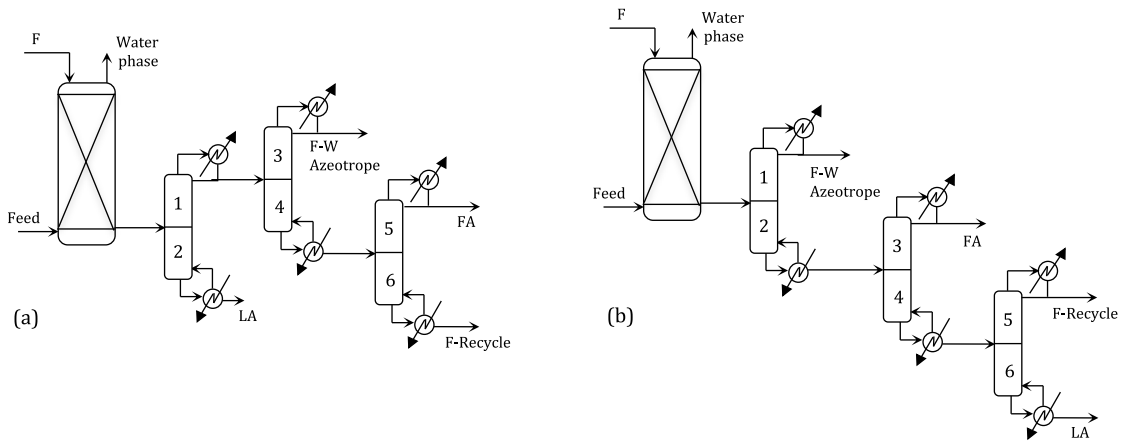

Fig. 1. Hybrid liquid-liquid ordinary distillation sequences proposed by: (a) Seibert [15], (b) Nhien [14].

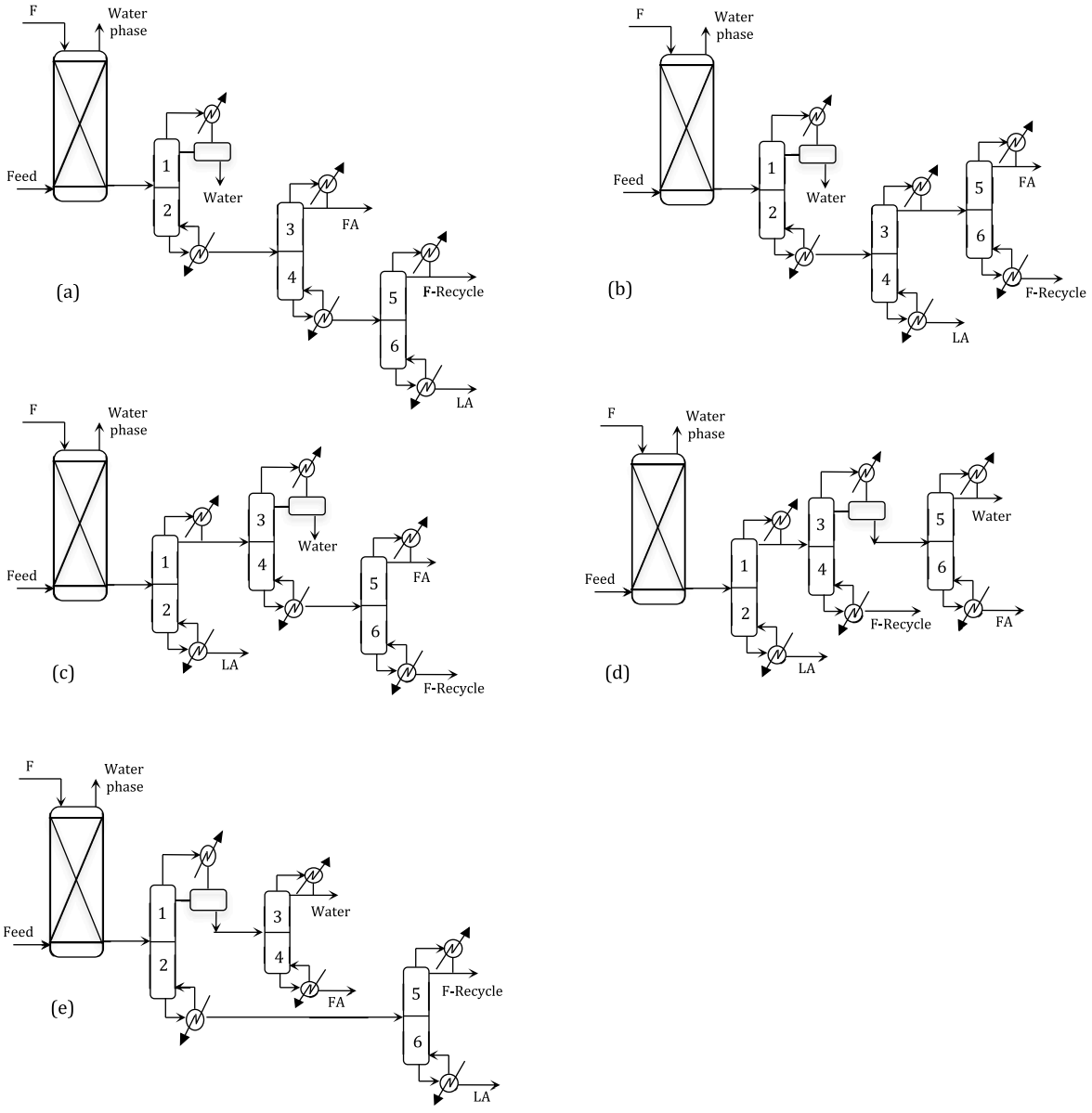

Fig. 2. Possible sequences for hybrid liquid-liquid extraction combined ordinary distillation.

simulator databank with available experimental data for the properties of the F-LA-FA system.

3. Design of hybrid liquid-liquid plus ordinary distillation configurations

Based on the distribution of the components' boiling point, with LA being the heaviest and water the lightest, the configurations of Fig. 2 can be renamed based on their separation order. Fig. 2a, where the components are separated from the lightest to the heaviest, is termed the direct sequence (DS), Fig. 2b the direct–indirect (DI), Fig. 2c the indirect-direct sequence (ID), Fig. 2d the indirect sequence (IS), and Fig. 2e the symmetrical sequence (SS).

All configurations were designed with Aspen Plus V12. The extractor was modeled by means of the rigorous countercurrent method "Extract" while "RadFrac" was used for the distillation columns. Sieve tray columns were considered together with kettle reboilers and fixed tube condensers. Tray efficiency and pressure drops were neglected. The decanter was modeled using the "Decanter" model for 2 liquid phases and no vapor. The NRTL-Hayden-O'Connell thermodynamic method was used to describe the liquid-liquid-vapor phase equilibria [14,29,30]. The available binary interaction parameters for the system were automatically retrieved from the Aspen Properties database, while those for LA-FA, LA-water, and LA-F were estimated using the UNIFAC method. The configurations were compared based on the associated TAC and the environmental impact ReCiPe method.

Data for the evaluation of the operating costs were retrieved from the Aspen Plus data bank. The capital costs were evaluated as equipment costs by the Aspen Process Economic Analyzer and annualized considering a 10-year project life. We also employed the "ReCiPe" methodology which is a method for life cycle impact assessment based on 18 midpoint indicators grouped into three categories: damage to human health, damage to the ecosystem, and damage to resource availability. The ReCiPe model is an improvement of the Eco-Indicator 99 already applied to compare different process alternatives [17,37,38]. The data used for the impact evaluation is reported in section S1 of the Supplementary Material.

Following Nhien et al. [14], a feed flow rate of 90000 kg h^{-1} at 25 °C and 2 atm was considered composed, on a weight basis, of 3% FA, 4% F, 7% LA with the rest being water. The purity targets were fixed based on the commercial request for 98% wt. of LA, 85% wt. of FA, and 99.9% wt. of F to be recirculated as extractive solvent. In this work, a purity constraint of 90% wt. for the water stream was additionally introduced.

The liquid-liquid extractor was designed to achieve a LA recovery of 99% on a mass basis in the extract stream. The number of stages and the solvent flow rate were used as optimization variables, resulting in a design with 36 stages and a solvent-feed ratio of 1.2. Details on the extractor optimization are reported in section S2 of the Supplementary Material. The design of the extractor remains unchanged for all configurations in Fig. 2.

The design of the distillation columns was performed considering the number of stages, feed location and reflux ratio as optimization variables. The overall recovery target for LA was set at 99.5% wt. based on the amount of LA in the furfural-rich stream obtained from the liquid-liquid extractor. The distillate (or residue) flow rate was defined based on material balances. Owing to the presence of the heteroazeotrope the decanter temperature also represents an optimization variable. Nhien et al. [14] proposed a temperature of 60 °C based on the fact that the F loss in the water phase is decreased by decreasing the temperature of the decanter inlet stream. Alcocer-Garcia et al. [30] used a value of about 98 °C that corresponds to the azeotropic temperature of the system. The definition of the decanter temperature can be performed by analyzing the mutual solubility data for the system F-water [39] reported in Fig. 3.

Based on the data shown on Fig. 3, the highest recovery of F is obtained at the lowest temperature. However, limiting the cooling utility to water available at 20 °C, considering a minimum driving force of 10 °C, and a FA recovery of 90%, the decanter temperature was set to 40 °C in order to satisfy the water purity constraint. The analysis of the decanter performance in the temperature range 30–80 °C is reported in section S3 of the Supplementary Material.

It should be noted that the columns' operating costs were evaluated considering medium-pressure steam for the columns performing the separation of the F-water azeotrope and the FA. The bottom temperature of the column separating LA is typically 249 °C. Taking into account that to high-pressure steam corresponds a temperature range 240–250 °C, its choice was considered not reasonable [40,41]. In contrast to Nhien et al. [14], hot oil available at 280 °C was chosen as a utility stream.

The design parameters, the energy consumption and the economic indexes for the configurations of Fig. 2 achieving the design constraints are shown in Table 1.

The DS and DI configurations reached the predefined purity and recovery targets but, for the ID case, even if the purity targets were

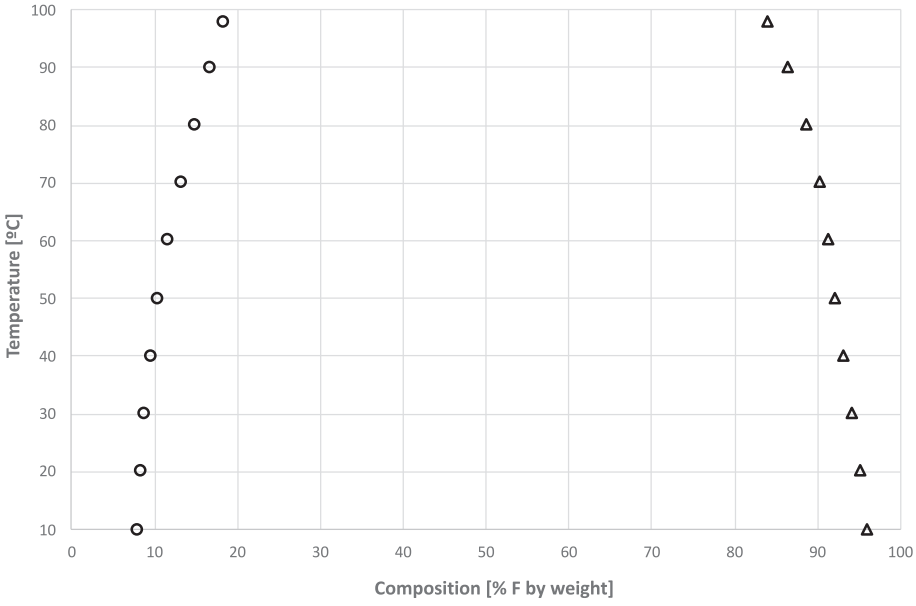

Fig. 3. Conjugated liquid phases composition-temperature diagram (o) water layer, (Δ) furfural layer.

Table 1
Design parameters and comparison indexes for the configuration of Fig. 2 reaching the purity targets.

		Fig. 2a (DS)	Fig. 2b (DI)	Fig. 2c (ID)
Column ½/3				
	Number of stages	20/35/18	20/18/30	18/19/30
	Feed stage	11/25/14	11/14/12	14/8/15
	Reflux ratio [mass base]	-/57.50/0.13	-/0.13/47.3	0.09/-/57
	Distillate [kg h^{-1}]	3432.02/ 322.50/ 104000	3432.02/ 104322/ 322.5	107755/ 3486.6/289
	Residue [kg h^{-1}]	110640/ 110317/ 6317.5	110640/ 6317.5/ 104000	6317.5/ 104268/ 103979
	Diameter [m]	2.68/1.91/ 3.21	2.68/3.24/ 1.75	4.14/1.86/ 1.75
	Condenser duty [MW]	2.51/4.10/ 14.30	2.51/14.48/ 3.39	17.76/2.27/ 3.38
	Reboiler duty [MW]	9.35/4.17/ 14.45	9.35/14.77/ 3.46	23.50/2.88/ 3.44
Purity [% wt.]				
	LA	98.20	98.20	98.20
	FA	85.10	85.10	85.10
	Water	91.30	91.30	90.30
	F-Recycle	99.90	99.90	99.90
Annualized capital cost [k$ yr^{-1}]		318	322	413
Operative cost [k$ yr^{-1}]		2685	2656	3292
TAC [k$ yr^{-1}]		3003	2978	3705
ReCiPe [Points yr^{-1}]		$1.35{\cdot}10^{8}$	$1.37{\cdot}10^{8}$	$2.2{\cdot}10^{8}$

satisfied, the recovery of FA was only 79% compared to the 90% achieved by DS and DI. This is due to the difference in temperature of the vapor stream leaving the column where the decanter is connected. In the DS and DI sequences the first column vapor head temperature is 100 °C, while in the second column of the ID sequence it is 112 °C with the consequence of a vapor richer in FA that is then lost in the water layer separated in the decanter.

Not surprisingly the IS and SS alternatives were not able to satisfy the purity and the recovery targets for the water and FA streams. For both IS and SS the water layer separated in the decanter is fed to the water-FA separation column. However, this stream is composed of 0.5% wt. of FA, 8.5% of F with water as the remainder, limiting the purity of FA achievable to about 74% wt.

The conclusion of this analysis is that the DS and DI configurations of Fig. 2a,b showed the best performances in terms of TAC and ReCiPe index without a significant difference between them to prefer one configuration over the other. This result validates the studies of Nihen et al. [14] that used the DS configuration to generate an alternative intensified version. However, the decision of Alcocer-Garcia et al. [30] to use the ID configuration of Fig. 2c as a reference and starting point for the generation of different intensified alternatives, appears not to be supported by a thorough analysis of the other simple column alternatives.

4. Analysis of the components' properties

It is well known that the design of unit operations based on phase equilibria is profoundly influenced by uncertainties in the thermophysical properties of the fluid systems. In fact, a different distribution of the components between two equilibrium phases results in different performances and different design parameters to reach the purity constraints set during the problem formulation. A case study on binary and ternary mixtures separated by distillation was presented by Wakeham et al. [42], which demonstrated the importance of the estimation methods and their integration in commonly used process simulators. The NRTL-Hayden O'Connell thermodynamic model, chosen for the simulations in the present work requires the components critical temperature, critical pressure, radius of gyration, dipole moment, as well as binary interaction parameters for each pair of chemicals.

The data retrieved from the Aspen Database for all the components except water, are reported in Table 2.

4.1. Critical properties, boiling point and dipole moment

The measurement of the critical properties is a significant challenge when the compound has the tendency to decompose. This is particularly true for LA and it is not surprising that the literature contains the results of several different approaches.

Chakraborti et al. [43], estimated the critical parameters of LA by applying a molecular simulation approach, and reported $T_c = 755$ K and $P_c = 30.57$ bar. Nikitin et al. [26], published experimental data obtained through the pulse-heating method, namely for the critical temperature 766 K and 53.1 bar for the critical pressure. The boiling point measured by Sah and Ma [44] is equal to 518.7 K, which is consistent with the range of values, 518–519 K reported in the CAS database [45]. This value is, however, over 10° lower than the one contained in the Aspen database.

For formic acid, according to Kudchadker et al. [46] the critical temperature is 588 ± 10 K. In the Dechema database a value of 581.2 K is recommended that is within the confidence interval provided by Kudchadker et al. [46]. Formic acid's critical pressure cannot be experimentally evaluated owing to the decomposition reactions observed in the experimentally-determined phase and reaction diagram reported by Montgomery et al. [47]. The Dechema database gives a value of 55.0 bar. While formic acid's boiling point is reported to be 373.87 K [48] in agreement with Aspen's database.

For furfural, critical properties of 670 K and 55.10 bar, respectively, were recommended by Kudchadker et al. [46]. However, it was stated that those are probably not experimental values. The value of the critical temperature agrees with the value provided both by Aspen and the Dechema. The latest data available for the critical pressure reported in the Dechema database is 58.9 bar while its boiling point was measured at 434.85 K [49] in agreement with the value used by Aspen.

Experimental values for the dipole moment are not available for LA but the values published for FA and F are in agreement with the Aspen database [50,51].

4.2. Binary interaction parameters

Binary interaction parameters extracted from Aspen database are summarized in Table 3.

Resk et al. [52] published P-x data for the LA-water system for a temperature of 60 °C and argued that the NRTL model fitted with their data also reproduced the T-x-y data published by Shilnikova and Ekimova [53]. This set of data is also included in the NIST database. Applying thermodynamic consistency tests, it is possible to obtain an overall data quality coefficient that is close to zero for a poor-quality data and close to unity in the case of good-quality data. This coefficient is evaluated based on the results of the Herington test, Van Ness test, Point test, Infinite dilution test, Equation of state test, and endpoint

Table 2
Components' properties critical temperature (T_c), critical pressure (P_c), boiling point (T_b), dipole moment (Dip), and radius of gyration (Rgyr) from the Aspen Database.

	T_c [K]	P_c [bar]	T_b [K]	Dip [debye]	Rgyr·10^{10} [m]
LA	738.00	40.20	530	1.33708	3.675
FA	588.00	58.10	373.71	1.41502	1.847
F	670.15	56.60	434.85	3.5975	3.35

Table 3
NRTL binary interaction parameter extracted from the Aspen database.

Component i	Component j	a_{ij}	a_{ji}	b_{ij}	b_{ji}
Water	FA	−2.5864	4.5156	725.017	−1432.08
Water	F	4.2362	−4.7563	−262.241	1911.42
Water	LA	0*	0*	1030.13*	−261.318*
FA	F	0	0	46.1655	289.216
LA	FA	0*	0*	−337.828*	569.5972*
LA	F	0*	0*	−336.725*	859.563*

* Estimated by UNIFAC method.

consistency test.

For the data available, the overall data quality coefficient is equal to 0.088 indicating it is not of good quality. For this reason, it was decided not to use those data to regress the binary coefficient for the water-LA pair. Details on the thermodynamic consistency test can be found in Wisniak et al. [54].

5. Impact of the components' properties on the hybrid liquid-liquid plus ordinary distillation design

The new set of properties reviewed in Section 4.1 and summarized in Table 4, were included in the Aspen Database and used in the simulation of the DS and DI configurations of Fig. 2a,b selected in Section 3 based on their TAC and ReCiPe index.

The effect of applying the data reported in Table 4 on the simulation for both DS and DI configurations was considerable: it was simply not possible to attain the purity and recovery targets for FA. This difficulty could be overcome by changing the number of stages or the reflux ratio of the column where the FA is recovered. However, if the effect on a column that was already operating is to be considered, it is easier to change the reflux ratio as a strategy. To reach the LA purity requirement, for both configurations was necessary to increase the reflux ratio by 2.0% when compared to the initial reflux ratio reported in Table 1. This corresponds also to an equivalent increase of the condenser and reboiler duties, OC, and TAC. The new TAC associated with the DS configuration is 3011 k$/yr while 2980 k$/yr was evaluated for the DI system. In both cases the ReCiPe index was not subjected to comparable variations.

6. Synthesis and design of intensified alternatives

The correspondence between the best simple column sequence and the best intensified alternative has been extensively discussed and proved for several different cases [31,55,56]. Based on this principle, the configurations DS and DI were examined to generate different intensified alternatives. Starting from the DS of Fig. 2a different alternatives can be generated by the substitution of reboilers and (or) condensers associated to non-product streams followed by different column section recombination techniques. Nevertheless, configurations obtained by elimination of the reboiler associated to the second distillation column have been discarded. This is because of the shift of the vapor boil-up for the third and second column to the reboiler associated with the heaviest compound and then to the hottest utility. More promising are those alternatives that are obtained by intensification of the first two distillation columns of the sequence leaving the third column unchanged. The configuration in Fig. 4a was obtained from the corresponding DS by removing the reboiler of the second column and rearranging the column sections in a way such that the FA is separated in an external stripping section connected to the first column by a thermal coupling. This alternative is classified as a thermodynamically equivalent configuration. Integrating the single stripping section, numbered as section 3 in Fig. 4a, into the first column, it is possible to obtain the divided wall configuration shown in Fig. 4b. This is the maximum level of intensification achievable based on the idea of leaving the column performing the separation of LA unchanged.

Intensification opportunities derived from the DI configuration of Fig. 2b are limited since it is not convenient to remove the first column reboiler and provide all the vapor boil-up through the reboiler associated with LA. Moreover, the possibility of substituting the second column condenser with a thermal coupling appears to be of limited impact. This configuration was already designed by Errico et al. [29] achieving only a 2% saving in the operating cost if compared to the DI configuration. For this reason, only the two configurations reported in Fig. 4 were examined further.

The design of the configurations in Fig. 4 followed the principle of column section recombination. It is based on the correspondence of configuration parameters, e.g. number of stages and feed locations of the intensified configurations, from the simple column sections from which they are derived [33,34]. For the scheme displayed in Fig. 4a it remains to evaluate the vapor-side stream that connects the first column with the second, while for the one in Fig. 4b the vapor split between the two sides of the wall needs to be specified. In both cases the minimum value that assures reaching the purity constrains was chosen. A summary of the intensified alternative performances in terms of TAC and ReCiPe index is reported in Table 5.

The results presented in Table 5 clearly demonstrate that both intensified configurations outperformed the DS of Fig. 2a from which they are derived. In particular, the thermodynamically equivalent and the configuration with a DWC (Fig. 4a and 4b, respectively) achieved a TAC reduction of about 11 %. It is also remarkable to observe that the configuration with the DWC achieved a reduction of about 8 % in the annualized capital costs owing to the high degree of intensification. In both cases an improvement in the environmental index was not observed. This is because the highest impact is associated with the light oil used in the reboiler associated with the LA stream, and in the cases considered it was left unchanged.

Table 4
The new set of properties updated in the Aspen Database and difference (Δ) with respect to the original value.

	T_c [K]	P_c [bar]	T_b [K]	ΔT_c [%]	ΔP_c [%]	ΔT_b [%]
LA	766.00	53.10	518.70	+3.8	+32.1	−2.3
FA	581.20	58.10	373.71	+1.2	0	0
F	670.15	58.90	434.85	0	+4.1	0

7. Conclusions

The separation of levulinic acid produced through biomass acid hydrolysis was examined by analyzing different hybrid flowsheets where liquid-liquid extraction was followed by ordinary distillation. It was proved that among all the possibilities only the hybrid direct, direct-indirect, and indirect-direct were able to achieve the purity target set. Nevertheless, the indirect-direct configuration was penalized not only because it had the highest TAC and environmental indexes compared to the other alternatives, but also because of the limitation of the maximum recovery of formic acid achievable. The selected configurations were further analyzed to study the influence of the thermophysical properties on the simulation results. For both configurations a 2% offset was observed in the purity required for the formic acid. The result shows the necessity for experimental data on thermophysical properties, especially

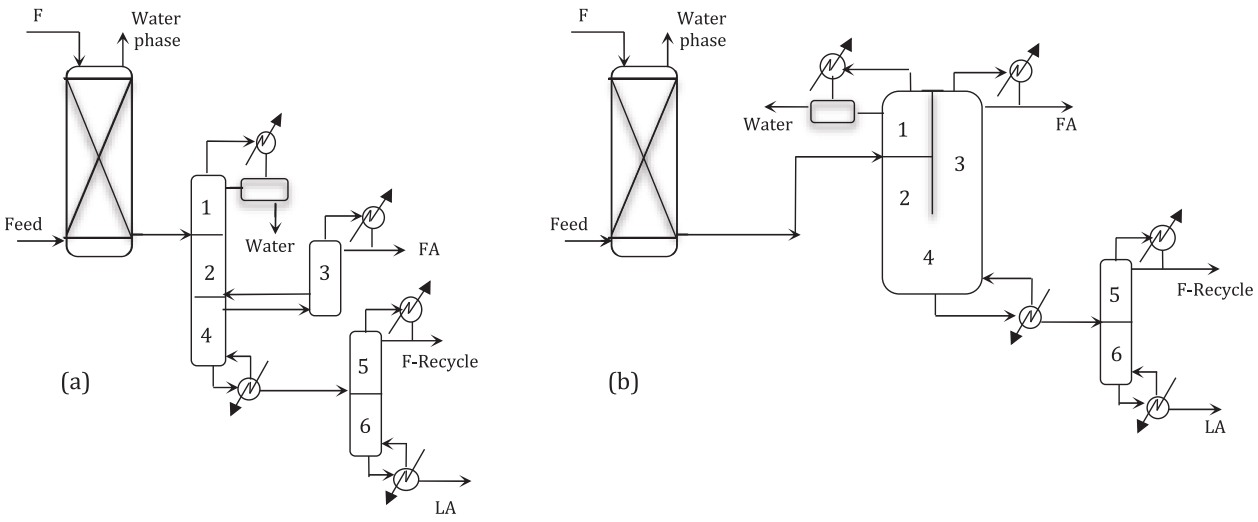

Fig. 4. Intensified configurations derived from the DS: thermodynamically equivalent configuration (a), configuration with a divided wall column (b).

Table 5
Performance indexes of the intensified configurations of Fig. 4.

	Fig. 4a	Fig. 4b
Annualized capital cost [k$ yr^{-1}]	306	293
Operative cost [k$ yr^{-1}]	2388	2392
TAC [k$ yr^{-1}]	2694	2685
ReCiPe [Points yr^{-1}]	$1.35{\cdot}10^{8}$	$1.35{\cdot}10^{8}$

for bioderived compounds where simulator databases mostly rely only on estimated data.

Intensified alternatives were finally examined with the aim to perform the separation more economically competitive and with a reduced environment impact. Two intensified alternatives were considered. The first, obtained introducing a thermal coupling and recombining the column sections, the second with a further intensification by introducing a divided wall column. Both alternatives showed promising results in terms of total annual costs by saving 11% compared to the direct configuration. No environmental benefit or penalty was observed for these alternatives and both of them represent a valuable option to make the large-scale production of levulinic acid closer to a practical reality.

CRediT authorship contribution statement

Stefania Tronci: Conceptualization, Methodology, Validation, Writing – review & editing. **Debora Garau:** Formal analysis, Investigation. **Roumiana P. Stateva:** Conceptualization, Methodology, Validation, Funding acquisition, Writing – review & editing. **Georgi Cholakov:** Conceptualization, Methodology, Validation, Writing – review & editing. **William A. Wakeham:** Conceptualization, Methodology, Validation, Writing – review & editing. **Massimiliano Errico:** Conceptualization, Methodology, Formal analysis, Software, Funding acquisition, Validation, Writing – original draft, Writing – review & editing.

Declaration of Competing Interest

The authors declare that they have no known competing financial interests or personal relationships that could have appeared to influence the work reported in this paper.

Data availability

Data will be made available on request.

Acknowledgement

This project has received funding from the European Union's Horizon 2020 research and innovation programme under the Marie Sklodowska-Curie grant agreement No 778168.

Appendix A. Supplementary data

Supplementary data to this article can be found online at https://doi.org/10.1016/j.seppur.2023.123166.

References

[1] U.S: Department of Energy. Top Value Added Chemicals from Biomass. Volume I-Results of Screening for Potential Candidates from Sugar and Synthesis Gas. T. Werpy and G. Petersen Editors, 2004.
[2] G. Cavinato, L. Toniolo, Levulinic acid synthesis via regiospecific carbonylation of methyl vinyl ketone or of its reaction products with hydrochloric acid or an alkanol or of a mixture of acetone with a formaldehyde precursor catalyzed by a highly active Pd-HCl system, J. Mol. Catal. 58 (1990) 251–267.
[3] R. Ballini, M. Petrini, Facile and inexpensive synthesis of 4-oxoalkanoic acids from primary nitroalkanes and acrolein, Synthesis 12 (1986) 1024–1026.
[4] H.L. Reid, Levulinic acid as a basic chemical raw material, Ind. Eng. Chem. 48 (1956) 1330–1341.
[5] A. Corma, S. Iborra, A. Velty, Chemical routes for the transformation of biomass into chemicals, Chem. Rev. 107 (2007) 2411–2502.
[6] K. Yan, C. Jarvis, J. Gu, Y. Yan, Production and catalytic transformation of levulinic acid: A platform for speciality chemicals and fuels, Renew. Sustain. Energy Rev. 51 (2015) 986–997.
[7] S.-H. Pyo, S.J. Glaser, N. Rehnberg, R. Hatti-Kaul, Clean production of levulinic acid from fructose and glucose in salt water by heterogeneous catalytic dehydration, ACS Omega 5 (2020) 14275–14282.
[8] A. Morone, M. Apte, R.A. Pandey, Levulinic acid production from renewable waste resources: Bottlenecks, potential remedies, advancements and applications, Renew. Sustain. Energy Rev. 51 (2015) 548–565.
[9] D. Di Menno Di Bucchianico, Y. Wang, J.-C. Buvat, Y. Pan, Moreno V. Casson, S. Leveneur, Production of levulinic acid and alkyl levulinates: a process insight, Green Chemistry 24 (2020) 614–646.
[10] B.A. Fachri, R.M. Abdilla, H.H. van de Bovenkamp, C.B. Rasrendra, H.J. Heeres, Experimental and kinetic modeling studies on the sulfuric acid catalyzed conversion of D-fructose to 5-hydroxymethylfurfural and levulinic acid in water, ACS Sustainable Chem. Eng. 3 (2015) 3024–3034.
[11] L.B. Woo, S.J. Young, K. Jeong, J. Choi, K.Y. Cho, S. Cho, K.-Y. Baek, Efficient production of levulinic acid using metal-organic framework catalyst: Role of Brønsted acid and flexibility, Chem. Eng. J. 444 (2022), 136566.
[12] A.A. Kiss, J.-P. Lange, B. Schuur, D.W.F. Brilman, A.G.J. van der Ham, S.R. A. Kersen, Separation technology – Making a difference in biorefineries, Biomass Bioenergy 95 (2016) 296–309.

[13] A.A. Kiss, J. Grievink, M. Rito-Palomares, A system engineering perspective on process integration in industrial biotechnology, Chem. Technol. Biotechnol. 90 (2015) 349–355.
[14] L.C. Nhien, N. Van Duc Long, M. Lee, Design and optimization of the levulinic acid recovery process from lignocellulosic biomass, Chem. Eng. Res. Des. 107 (2016) 126–136.
[15] F. Seibert, A method of recovering levulinic acid. WIPO Patent WO/2010/030617 A1, 2010.
[16] D.K. Babi, C.M. Sales, R. Gani, Fundamentals of Process Intensification: A Process Systems Engineering View, in: J. Gabriel (Ed.), Process Intensification in Chemical Engineering, Springer, Segovia-Hernández, Adrián Bonilla-Petriciolet, 2016, pp. 7–33.
[17] M. Errico, E. Sanchez-Ramirez, J.J. Quiroz-Ramìrez, B.-G. Rong, J.G. Segovia-Hernandez, Multi Objective Optimal Acetone-Butanol-Ethanol (ABE) Separation Systems using Liquid-Liquid Extraction Assisted Divided Wall Columns, Ind. Eng. Chem. Res. 56 (2017) 11575–11583.
[18] E. Sanchez-Ramirez, H. Alcocer-Garcia, J.J. Quiroz-Ramirez, C. Ramirez-Marquez, J.G. Segovia-Hernandez, S. Hernandez, M. Errico, A.J. Castro-Montoya, Control properties of hybrid distillation processes for the separation of biobutanol, J. Chem. Technol. Biotechnol. 92 (2017) 959–970.
[19] M.A. Aviles, J. Saucedo-Luna, J.G. Segovia Hernandez, S. Hernandez, F. Gomez-Castro, A.J. Castro-Montoya, Dehydration of bioethanol by hybrid process liquid-liquid extraction/extractive distillation, Ind. Eng. Chem. Res. 51 (2012) 5847–5855.
[20] M. Vazquez-Ojeda, J.G. Segovia-Hernandez, S. Hernandez, A. Hernandez-Aguirre, A.A. Kiss, Design and optimization of an ethanol dehydration process using stochastic method, Sep. Purif. Technol. 105 (2013) 90–97.
[21] M. Errico, Process synthesis and intensification of hybrid separations, in: B.-G. Rong (Ed.), Process Synthesis and Process Intensification: Methodological Approaches, De Gruyter, Berlin, Boston, 2017, pp. 182–212.
[22] W. Wakeham, M.J. Assael, The dangerous nexus of process simulation, molecular modelling and physical reality, Bul. Chem. Commun. 51 (2019) 9–21.
[23] M.J. Assael, A. Leipertz, E. MacPherson, Y. Nagasaka, C.A. Nieto de Castro, R. A. Perkins, K. Ström, E. Vogel, W.A. Wakeham, Transport property measurements on the IUPAC sample of 1,1,1,2-Tetrafluoroiethane (R134a), Int. J. Thermophys. 21 (2000) 1–22.
[24] G. Tertsinidou, M.J. Assael, W.A. Wakeham, The apparent thermal conductivity of liquids containing solid particles of nanometer dimensions: A critique, Int. J. Thermophys. 36 (2015) 1367–1395.
[25] H. Ariba, Y. Wang, C. Devouge-Boyer, R.P. Stateva, S. Leveneur, Physicochemical properties for the reaction systems: levulinic acid, its esters, and γ-valerolactone, J. Chem. Eng. Data 65 (2020) 3008–3020.
[26] E.D. Nikitin, A.P. Popov, N.S. Bogatishcheva, M.Z. Faizullin, Critical temperatures and pressures, heat capacities, and thermal diffusivities of levulinic acid and four n-alkyl levulinates, J. Chem. Thermodynamics 135 (2019) 233–240.
[27] T. Brouwer, M. Blahusiak, K. Babic, B. Schuur, Reactive extraction and recovery of levulinic acid, formic acid and furfural from aqueous solution containing sulphuric acid, Sep. Purif. Technol. 185 (2017) 186–195.
[28] A. Kumar, D.Z. Shende, K.L. Wasewar, Extractive separation of levulinic acid using natural and chemical solvents, Chem. Data Collect. 28 (2020), 100417.
[29] M. Errico, R.P. Stateva, S. Leveneur, Novel intensified alternatives for purification of levulinic acid recovered from lignocellulosic biomass, Processes 9 (2021) 490.
[30] H. Alcocer-Garcia, J.G. Segovia-Hernandez, O.A. Prado-Rubio, E. Sanchez-Ramirez, J.J. Quiroz-Ramirez, Multi-objective optimization of intensified processes for the purification of levulinic acid involving economic and environmental objectives, Chem. Eng. Process. 136 (2019) 123–137.
[31] M. Errico, B.-G. Rong, G. Tola, I. Turunen, A method for systematic synthesis of multicomponent distillation systems with less than N-1 columns, Chem. Eng. Process. 48 (2009) 907–920.
[32] B.-G. Rong, M. Errico, Synthesis of intensified simple column configurations for multicomponent distillations, Chem. Eng. Process. 62 (2012) 1–17.
[33] M. Errico, P. Pirellas, C.E. Torres-Ortega, B.-G. Rong, J.G. Segovia-Hernandez, A combined method for the design and optimization of intensified distillation systems, Chem. Eng. Process. 85 (2014) 69–76.
[34] M. Errico, B.-G. Rong, C.E. Torres-Ortegas, J.G. Segovia-Hernandez, The importance of the sequential synthesis methodology in the optimal distillation sequences design, Comput. Chem. Eng. 62 (2014) 1–9.
[35] M. Errico, B.-G. Rong, Systematic synthesis of intensified distillation systems, in: J. G. Segovia-Hernandez, A. Bonilla-Petriciolet (Eds.), Porcess Intensification in Chemical Engineering. Design Optimization and Control, Springer International Publishing Switzerland, 2016, pp. 35–64.
[36] R.W. Thompson, C.J. King, Systematic synthesis of separation schemes, AIChE J 18 (1972) 941–948.
[37] C. Gonzalez-Navarrete, E. Sanchez-Ramirez, C. Ramirez-Marquez, S. Hernandez, E. Cossio-Vergas, J.G. Segovia-Hernandez, Innovative Reactive distillation process for the sustainable purification of lactic acid, Ind. Eng. Chem. Res. 61 (2022) 621–637.
[38] R. Brunet, G. Guillen-Gosalbez, L. Jimenez, Cleaner design of single-product biotechnological facilities through the integration of process simulation, multiobjective optimization, life cycle assessment, and principal component analysis, Ind. Eng. Chem. Res. 51 (2012) 410–424.
[39] A.P. Dunlop, F.N. Peters, The Furans, Reinhold Publishing Corporation, NY, U.S.A, 1953.
[40] W.D. Seider, D.R. Lewin, J.D. Seader, S. Widagdo, R. Gani, K.M. Ng, P Product and Process Design Principles. Synthesis, Analysis, and Evaluation, John Wiley & Sons Inc., New York, 2017.
[41] R. Turton, R.C. Bailie, W.B. Whiting, Shaeiwitz. Analysis, Synthesis, and Design of Chemical Processes. Boston, Pearson Education, Inc., 2009.
[42] W.A. Wakeham, G. St. Cholakov, R.P. Stateva, Consequences of property errors on the design of distillation columns. Fluid Phase Equilibria, 185 (2001) 1-12.
[43] T. Chakraborti, A. Desouza, J. Adhikari, Prediction of thermodynamic properties of levulinic acid via molecular simulation techniques, ACS Omega 3 (2018) 18877–18884.
[44] P.P.T. Sah, S.-Y. Ma, Levulinic acid and its esters, J. Am. Chem. Soc. 52 (1930) 4880–4883.
[45] CAS Database, available online at: https://www.cas.org/support/documentation/cas-databases (consulted on September 22nd 2022).
[46] A.P. Kudchadker, D. Ambrose, C. Tsonopoulos, Vapor-liquid critical properties of elements and compounds. 7. Oxygen compounds other than alkanols and cycloalkanols, J. Chem. Eng. Data 46 (2001) 457–479.
[47] W. Montgomery, J.M. Zaug, W.M. Howard, A.F. Goncharov, J.C. Crowhurst, R. Jeanloz, Melting curve and high-pressure chemistry of formic acid to 8 GPa and 600 K, J. Phys. Chem. B 109 (41) (2005) 19443–19447.
[48] CAMEO Chemicals, Database of Hazardous Materials, available online at: https://cameochemicals.noaa.gov (consulted on September 22nd 2022).
[49] The Chemistry and Technology of Furfural and its Many By-Products. Sugar Series, Volume 13, Edited by Karl J. Zeitsch, 2000, Elsevier (doi.org/10.1016/S0167-7675(00)80001-9).
[50] Kim H., Keller R., Gwinn W.d. (1962) Dipole moment of formic acid, HCOOH and HCOOD. J. Chem Phys. 37, 2748.
[51] P.T. Narasimhan, Dipole moments of some heterocyclic compounds, J. Indian Inst. Sci. 37 (1955) 30–34.
[52] A.J. Resk, L. Peereboom, A.K. Kolah, D.J. Miller, C.T. Lira, Phase equilibria in systems with levulinic acid and ethyl levulinate, J. Chem. Eng. Data 59 (2014) 1062–1068.
[53] L.L. Shiĺnikova, N.V. Ekimova, Liquid-vapor equilibrium in the system water + levulinic acid. Gidroliz. Lesokhim. Prom-st., 21 (1968) 15-16.
[54] J. Wisniak, A. Apelblat, H. Segura, An assessment of thermodynamic consistency tests for vapor-liquid equilibrium data, Phys. Chem. Liq. 35 (1997) 1–58.
[55] B.-G. Rong, A. Kraslawski, Partially thermally coupled distillation systems for multicomponent separations, AIChE J. 49 (2003) 1340–1347.
[56] M. Errico, G. Tola, B.-G. Rong, D. Demurtas, I. Turunen, Energy saving and capital cost evaluation id distillation column sequences with a divided wall column, Chem. Eng. Res. Des. 87 (2009) 1649–1657.